Galactic Dynamics in the Era of Large Surveys
Proceedings IAU Symposium No. 353, 2019
M. Valluri & J. A. Sellwood, eds.

doi:10.1017/S1743921319008536

Constraining the Milky Way non-axisymmetries with Gaia

B. Famaey[1], G. Monari[1], A. Siebert[1], O. Bienaymé[1], R. Ibata[1], C. Wegg[2] and O. Gerhard[3]

[1]Université de Strasbourg, CNRS UMR 7550, Observatoire astronomique de Strasbourg
email: benoit.famaey@astro.unistra.fr

[2]Université Côte d'Azur, Observatoire de la Côte d'Azur, CNRS, Laboratoire Lagrange

[3]Max-Planck-Institut für extraterrestrische Physik, Garching

Abstract. The unprecedented amount and accuracy of kinematic data from the second release of the Gaia mission have started revolutionizing our understanding of the dynamics of the Milky Way disk. The detailed stellar velocity field in the Galactic disk should allow us to constrain with unprecedented precision the parameters of the non-axisymmetric modes of the disk. We present here the status of our current modelling efforts in this area, and their implication on the dynamics of the Galactic bar in particular.

Keywords. Galaxy: kinematics and dynamics, Galaxy: disk, Galaxy: structure

1. Action-angle variables and perturbation theory

The natural phase-space coordinates to describe stellar dynamics in the Galaxy are action-angle variables. In an axisymmetric potential within a cylindrical coordinate system (R, ϕ, z), the three natural action coordinates to use are J_R, J_ϕ, J_z and their canonically conjugate angle variables evolve linearly with time as $\theta_i(t) = \theta_{i0} + \omega_i t$, where the fundamental orbital frequencies ω_i are functions of the actions. In an equilibrium configuration, the stellar angle coordinates are phase-mixed on orbital tori that are labelled by the three actions, and the unperturbed phase-space distribution function (DF), f_0, is a function of actions alone (a.k.a. Jeans theorem). The angle coordinates, on the other hand, indicate where each star lies along its orbit, and in particular the angle θ_ϕ is closely related to the azimuth ϕ of the star in the cylindrical coordinate system.

Let us then consider a perturbing potential Φ_1 (from, e.g., the Galactic bar or from some spiral mode), rotating with a pattern speed Ω_p. A 2D resonance with the perturber occurs when the fundamental orbital frequencies ω_R and ω_ϕ are such that

$$l\omega_R + m(\omega_\phi - \Omega_p) = 0. \tag{1.1}$$

Far from resonances, the orbital tori on which regular orbits are confined are just distorted by the small perturbing potential Φ_1. This problem can also be treated by linearizing the collisionless Boltzmann equation. But close to resonances, orbital tori are radically modified. As a consequence, for each resonance, one should define a new set of actions and angles suitable to describe the orbits. The key to this problem, which we investigated in Monari *et al.* (2017), is to make two consecutive canonical transformations in order to find the relevant action variables to use in the resonant region. Once this is done, one can populate the new tori through phase-averaging the original unperturbed DF f_0 over the new resonant tori. We limit ourselves to the 2D planar case in the following.

The first time-dependent canonical transformation disentangles the slow and fast motion near a given $m:l$ resonance,

$$\theta_{\rm s} = l\theta_R + m(\theta_\phi - \Omega_p t), \quad \theta_{\rm f} = \theta_R, \quad J_{\rm s} = J_\phi/m, \quad J_{\rm f} = J_R - (l/m)J_\phi. \tag{1.2}$$

The angle $\theta_{\rm s}$ is said to be slow because in the unperturbed case, the definition of the resonance is such that it indeed evolves very slowly. The next step is to replace the real Hamiltonian of the system by a Hamiltonian averaged over the fast variable, in order to study the evolution of the slow angle and slow action, by making the fast action $J_{\rm f}$ an approximate integral of motion. For each $J_{\rm f}$, we can then define $J_{\rm s,res}$ as the $J_{\rm s}$ satisfying $\Omega_{\rm s}(J_{\rm s}, J_{\rm f}) = 0$. We then expand the Hamiltonian in $J_{\rm s}$ around $J_{\rm s,res}$ to obtain a one-dimendional *pendulum* Hamiltonian.

We then make a second canonical transformation to go from the slow angle and action to the actual corresponding *pendulum* action and angle $(J_{\rm p}, \theta_{\rm p})$. The trapped DF should thus be written as a function $f_{\rm tr}(J_{\rm f}, J_{\rm p})$.

Assuming that the perturbation has been long-lived enough for phase-mixing to be efficient, the natural outcome for the trapped DF is then

$$f_{\rm tr}(J_{\rm f}, J_{\rm p}) = \frac{1}{2\pi}\int_0^{2\pi} f_0(J_{\rm f}, J_{\rm s}(J_{\rm p}, \theta_{\rm p}))\mathrm{d}\theta_{\rm p} \tag{1.3}$$

where f_0 is the original unperturbed DF.

2. The local effects of the bar: *Hercules*, the horn and the hat

The second data release from the Gaia mission has revealed a rich network of substructures in local phase-space with unprecedented details, displaying multiple clearly defined ridges in velocity space, and even vertical velocity disturbances. As far as in-plane motions are concerned, it is interesting to consider the distribution of stars in the space of axisymmetric actions. Trick *et al.* (2019) produced such plots in various volumes around the Sun. For local stars ($d < 200$ pc), they revealed several prominent ridges in the radial action distribution, among which a double-peak at the lowest border of the local azimuthal action (angular momentum) distribution, corresponding to the well-known *Hercules* moving group at low azimuthal velocities, and one at high angular momentum, corresponding to an arch at high velocities covering the velocity ellipsoid from above (the 'hat').

In Monari *et al.* (2019a), we used the method developed in Monari *et al.* (2017) and described in Sect. 1 to study the response of the Galactic disc DF to the large bar Galactic potential model developed by Portail *et al.* (2017), with pattern speed 39 km $\rm s^{-1}kpc^{-1}$. Extracting from this potential model the Fourier modes of the bar, we have shown that the $m = 2$, $m = 4$, and $m = 6$ resonances deform the disc DF in ways that resemble those shown by Gaia around the Sun. The $m = 2$ mode corotation and 2:1 resonance can be tentatively associated to features like the *Hercules* moving group (corotation) and the 'hat' (2:1, albeit slightly less marked than in the data). Interestingly, the 6:1 resonance of the $m = 6$ mode corresponds to the so called 'horn' feature of the local velocity space.

While it is clear that effects from spiral arms and incomplete phase-mixing related to external perturbations should also play a role in shaping the complex kinematics, we demonstrated that the bar alone can create multiple prominent ridges in local velocity and action space. The direct comparison between the model and the heliocentric velocity features in the data favours a small peculiar tangential velocity of the Sun. However, a small change of the circular velocity curve in the model can result in agreement with the data and a peculiar velocity of the Sun in line with previous estimates in the literature.

https://doi.org/10.1017/S1743921319008536 Published online by Cambridge University Press

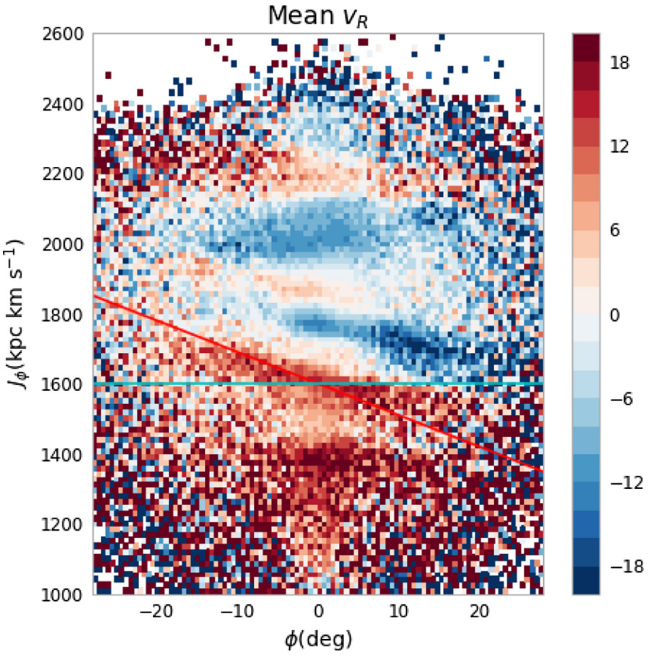

Figure 1. Mean v_R in the (ϕ, J_ϕ) space obtained for stars from 1535484 Gaia DR2 RVS stars inside an annulus of ± 0.2 kpc around the Sun. The red line corresponds to the theoretical slope of *Hercules* expected for the corotation, -8 km s^{-1} kpc deg^{-1}, and the blue line to 0 km s^{-1} kpc deg^{-1} expected for the outer Lindblad resonance of a dynamically old bar. The blue horn feature right above *Hercules* has a strongly negative radial velocity at positive azimuth which disappears at negative azimuth, favoring a resonance with a high order mode.

3. Following *Hercules* in azimuth

While we showed that the barred Galactic model of Portail *et al.* (2017) can reproduce most of the observed features of the local velocity and action space, many of these can be explained by different combinations of non-axisymmetric perturbations, making their modelling degenerate, as recently shown by, e.g., Hunt *et al.* (2019). For instance, if the Sun is located just outside of the bar's outer 2:1 Lindblad resonance, *Hercules* is caused by the linear deformation of velocity space. Then, orbits trapped at the resonance are responsible for the 'horn' feature which delineates the boundary of the linear deformation zone, whilst if the Sun is located just outside the bar's co-rotation radius, as in the model of Portail *et al.* (2017), orbits *trapped* at corotation are responsible for *Hercules* and the 'horn' corresponds to stars trapped at the 6:1 resonance.

In Monari *et al.* (2019b), we attempted to follow the *Hercules* ridge as a function of azimuth to disentangle the effect of different resonances that could cause it. For this, let us consider a set of trapped orbits at the azimuth of the Sun within a small annulus of Galactocentric radii around the Sun (with different radial angles θ_R, but with similar angular momentum J_ϕ). We then evolve these orbits in time. The radial angle is a fast-varying variable ($\theta_R = \theta_f$), hence once the radial angles have varied by a small amount, e.g. $\sim \pi/4$, the slow angle θ_s and action J_s will have varied only very little. If we consider the $(l, m) = (1, 2)$ outer Lindblad resonance of the bar, Eq. 1.2 hereabove then implies that the azimuthal angle in the bar frame will have evolved in magnitude by $\sim \pi/8 = 22.5°$, whith almost constant θ_s and J_s. Hence we expect that orbits trapped at the outer Lindblad resonance will remain at almost constant $J_\phi = 2J_s$ over that range of azimuthal angles to the bar. Note that this heuristic argument becomes less and less

https://doi.org/10.1017/S1743921319008536 Published online by Cambridge University Press

valid for resonances with much larger values of m. On the other hand, if we consider the $(l, m) = (0, 2)$ corotation resonance, the angle to the bar becomes half the slow angle because $l = 0$. This means that any significant variation of this angle to the bar will be accompanied by a similar variation (and even larger by a factor of 4) in the angular momentum J_ϕ. Hence we expect the angular momentum of orbits trapped at corotation to significantly vary with azimuth, while this is not the case for stars trapped at the outer Lindblad resonance. In Monari *et al.* (2019b), we confirmed this heuristic argument by making a quantitative evaluation of the trapped DF using the method described in Sect. 1 and in Monari *et al.* (2017). The shift with azimuth of the angular momentum corresponding to *Hercules* in the Portail *et al.* (2017) model is -8 km s^{-1} kpcdeg^{-1}, while there is basically no shift at the 2:1 outer Lindblad resonance. These trends are plotted as a red line and a blue line on Fig. 1, where Gaia data are overplotted. The only way out for an explanation based on the outer Lindblad resonance would be if the bar is still fairly young, such that orbits are still far from phase-mixed in the bar frame. This could cause a significant variation of the angular momentum with azimuth even at the outer Lindblad resonance, but only within the first $\sim$2 Gyr after bar formation

4. Conclusion

The optimal exploitation of the exquisite data from the Gaia mission involve the construction of a dynamical model of the Milky Way based on a multi-component stellar phase-space DF obeying the collisionless Boltzmann equation. The natural phase-space coordinates to use for this are action-angle variables, such that the phase-space DF at equilibrium is a function of actions alone. These variables are also ideal for perturbation theory. In Monari *et al.* (2017), we devised a method to treat the response of such a DF to a rotating perturber potential, such as the bar or a spiral mode, at resonances where treatments based on linearizing the collisionless Blotzmann equation diverge. In Monari *et al.* (2019a), we used this method to study the response of the Galactic disc DF to the large bar Galactic potential model developed by Portail *et al.* (2017), with pattern speed 39 km s^{-1}kpc^{-1}, demonstrating that the bar alone can create multiple prominent ridges in local velocity and action space, including *Hercules* (corotation resonance), the 'horn' (6:1 resonance) and the 'hat' (2:1 outer Lindblad resonance). However, many of these can be explained by different combinations of non-axisymmetric perturbations, making their modelling degenerate. In Monari *et al.* (2019b), we thus attempted to follow the *Hercules* ridge as a function of azimuth to disentangle the effect of different resonances that could cause it. Our findings reinforce the case for a corotation origin of *Hercules* in the case of a dynamically old bar (>2 Gyr). There however remain numerous intriguing features in the observed angular momentum vs. azimuth plot (Fig. 1), to understand in future works, and it is clear that spiral arms and the recent interaction of the disk with external perturbers might also play a role in interpreting these kinematic features. Data in a larger range of azimuths with future Gaia data releases will also allow all these potential effects to be tested further.

References

Hunt, J., Bub, M., Bovy, J., Mackereth, T., Trick, W., & Kawata, D. 2019, arXiv:1904.10968
Monari, G., Famaey, B., Fouvry, J.-B., & Binney, J. 2017, *MNRAS*, 471, 4314
Monari, G., Famaey, B., Siebert, A., Wegg, C., & Gerhard, O. 2019a, *A&A*, 626, A41
Monari, G., Famaey, B., Siebert, A., Bienaymé, O., Ibata, R., Wegg, C., & Gerhard, O. 2019b, arXiv:1908.01318
Portail, M., Gerhard, O., Wegg, C., & Ness, M. 2017, *MNRAS*, 465, 1621
Trick, W., Coronado, J., & Rix, H.-W 2019, *MNRAS*, 484, 3291

https://doi.org/10.1017/S1743921319008536 Published online by Cambridge University Press